

# Inorganic Nanotubes: A Novel Platform for Nanofluidics

JOSHUA GOLDBERGER, RONG FAN, AND PEIDONG YANG\*

*Department of Chemistry, University of California, Materials Science Division, Lawrence Berkeley National Laboratory, Berkeley, California 94720*

Received September 22, 2005

## ABSTRACT

Templating approaches are being developed for the synthesis of inorganic nanotubes, a novel platform for nanofluidics. Single crystalline semiconductor GaN nanotubes have been synthesized using an epitaxial casting method. The partial thermal oxidation of silicon nanowires leads to the synthesis of silica nanotubes. The dimension of these nanotubes can be precisely controlled during the templating process. These inorganic nanotubes can be integrated into metal–oxide solution field effect transistors (MO-SolFETs), which exhibit rapid field effect modulation of ionic conductance. These nanofluidic devices have been further demonstrated to be useful for single-molecule sensing, as single DNA molecules can be readily detected either by charge effect or by geometry effect. These inorganic nanotubes will have great implications in subfemtoliter analytical technology and large-scale nanofluidic integration.

## Introduction

Carbon nanotubes were one of the first reported one-dimensional (1D) nanoscale materials, synthesized through bottom-up processes.<sup>1</sup> This single discovery has blossomed into an entire field of research devoted to the synthesis, properties, assembly, and application of carbon nanotubes, as well as other 1D materials, including semiconductor nanowires.<sup>2</sup> The usefulness of these materials lies not just in the direct miniaturization of micrometer-scale devices. Rather, there has been wide-

Joshua Goldberger was born in Akron, OH (1979). He received his B.Sc. in Chemistry in 2001 from The Ohio State University. He is currently working toward his Ph.D. in Inorganic Chemistry from the University of California, Berkeley, under the supervision of Peidong Yang with a National Science Foundation Graduate Research Fellowship. His main areas of research include the synthesis and properties of inorganic nanotubes, as well as the fabrication of electronic devices with these and other 1D nanomaterials.

Rong Fan received his B.S. (1999) and M.S. (2001) in chemistry from the University of Science and Technology of China. He is currently a Ph.D. candidate in materials chemistry at UC Berkeley. His interests include nanostructured semiconductors for thermoelectrics, the fundamentals of inorganic nanotube nanofluidics, and its application in single biomolecule sensing and reactions.

Peidong Yang received a B.S. in chemistry from University of Science and Technology of China in 1993 and a Ph.D. in chemistry from Harvard University in 1997. He did postdoctoral research at University of California, Santa Barbara, before joining the faculty in the department of Chemistry at the University of California, Berkeley, in 1999. He is the recipient of an Alfred P. Sloan research fellowship, the Arnold and Mabel Beckman Young Investigator Award, the National Science Foundation Young Investigator Award, the MRS Young Investigator Award, the Julius Springer Prize for Applied Physics, and the ACS Pure Chemistry Award. His main research interest is in the area of one-dimensional semiconductor nanostructures and their applications in nanophotonics, energy conversion, and nanofluidics. More about the Yang group research can be found in <http://www.cchem.berkeley.edu/~pdygrp/main.html>.

spread interest in understanding the influence of the nanometer size scale, the surface, and the dimensionality on the materials' physical properties (electronic, optical, mechanical, thermal etc.).

In this Account, we would like to introduce the concept of inorganic nanotubes as a new class of 1D nanostructures distinct from pure inorganic nanowires and carbon nanotubes in two ways. First, the resultant physical properties and electronic structure combine characteristics of both two-dimensional (2D) and 1D materials. A semiconductor nanotube can be thought of as a thin film rolled into a tube. Therefore, one degree of dimensionality is determined by the overall diameter, and another degree is determined by the shell thickness. One should be able to tune the properties of these nanotubes by accurately controlling these dimensions. Second, these hollow nanotubes can serve as nanoscale containers or pipes to deliver fluids and molecular species and are excellent building blocks for the construction of large-scale nanofluidic systems. We will show that these nanofluidic systems are fundamentally different from their microscale counterparts due to influence of their small sizes and the surface chemistry of these structures, therefore allowing the creation of solution-based transistors.

## Rational Synthesis of Inorganic Nanotubes

Since the discovery of carbon nanotubes in 1991 by Iijima, there have been significant research efforts devoted to nanoscale tubular forms of various solids,<sup>3–8</sup> including boron nitride, vanadium oxide, chalcogenides, bismuth, and NiCl<sub>2</sub>. The rule of thumb for the formation of tubular nanostructure is that the desired nanotubular material must have a layered or anisotropic crystal structure. There are reports of nanotube formation of solids lacking layered crystal structures, such as silica, alumina, silicon, and metals, through templating of carbon nanotubes or porous membranes.<sup>9,10</sup> These nanotubes, however, are either porous, amorphous, or polycrystalline or exist only in ultrahigh vacuum.<sup>11</sup> Many of these early techniques rely on wet chemistry at low temperatures, which therefore makes it difficult to synthesize high-quality, single-crystalline nanotubes with desired functionalities. The growth of robust nonporous nanotubes with uniform inner diameters would be advantageous in potential nanoscale electronics, optoelectronics, and biochemical sensing applications.

Our synthetic approach for nanotubular materials requires the use of nanowires as templates for the creation of core–sheath heterostructures, followed by the selective etching of the inner nanowire core. This core–sheath heterostructure can be formed in two ways. The first process requires the deposition of the desired nanotubular sheath materials using conventional thin-film deposition techniques. Alternatively, the existing nanowire templates can be partially converted using the proper chemistry to produce a core–sheath structure. In both processes, the

\* E-mail: p\_yang@berkeley.edu.

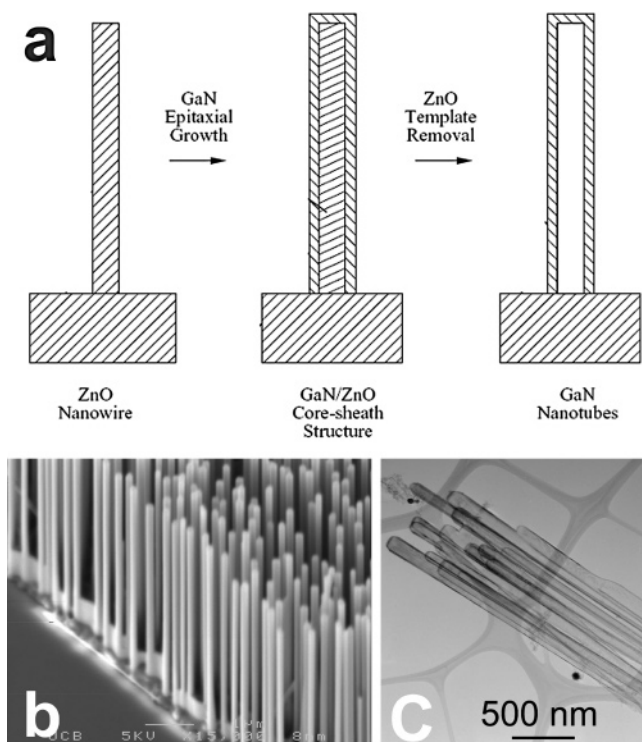


**FIGURE 1.** (a) Epitaxial casting approach to synthesize single-crystalline GaN nanotube arrays from ZnO nanowire templates, (b) SEM micrograph of the ZnO nanowire array, and (c) TEM micrograph of the resultant GaN nanotubes.

nanowire and nanotube material must have different chemical reactivities so that the inner core can be selectively removed. Additionally, the core and sheath materials must exist in epitaxial registry to obtain single-crystalline nanotubular materials.

We employed the first “epitaxial casting” process to synthesize single-crystalline GaN nanotubes.<sup>12</sup> As depicted in Figure 1a, ZnO nanowires are used as templates for the deposition of GaN thin films using metal–organic chemical vapor deposition (MOCVD). The ZnO nanowires can be easily etched away either in acidic solutions or via a high-temperature reduction step. Because ZnO and GaN both have a wurtzite crystal structure with similar lattice constants (<2% difference in the  $a, b$  parameters and <0.5% difference in the  $c$  parameter), this approach allows us to produce single-crystalline GaN nanotubes by exploiting this epitaxial relationship. Figure 1b,c shows scanning electron microscope (SEM) and transmission electron microscope (TEM) images of the ZnO nanowires and GaN nanotubes after etching away the ZnO nanowires, respectively. These nanotubes have inner diameters that are equal to the diameter of the starting ZnO nanowire template (30–200 nm), and thicknesses that can be controlled by adjusting the deposition time. This was the first single-crystalline nanotube created from a material that does not have a bulk layered crystal structure. The successful preparation of single crystalline GaN nanocapillaries using this “epitaxial casting” approach suggests that it is possible to prepare single-crystalline nanocapillaries of inorganic solids that have nonlayered crystal structures. This new class of semiconductor nano-

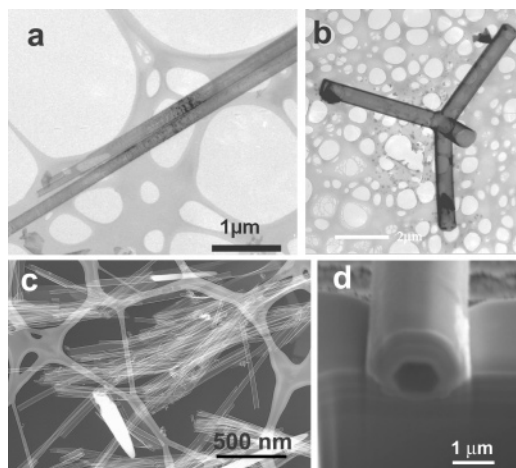


**FIGURE 2.** SEM and TEM images of various nanotube materials that have been produced using nanowires as templates: (a) TEM micrograph of single-crystalline Mn-doped GaN nanotubes; (b) TEM image of branched silica nanotubes templated from ZnO tetrapods; (c) TEM image of amorphous  $\text{TiO}_2$  nanotubes; (d) SEM micrograph of a multilayered  $\text{Si/SiO}_2$  nanotube.

tubes/nanocapillaries could offer great opportunities for further fundamental research as well as technological applications in nanoscale electronics and optoelectronics. Particularly of importance is (1) robustness of these semiconductor nanotubes, (2) uniform inner diameter, and (3) that the inner wall can be readily functionalized and both ends of the tubes can be made accessible to a fluid reservoir for quantitative nanofluidic measurement.

This nanotube synthesis generally requires three essential elements: a nanowire template, a conformal coating technique, and a selective etching step. Over the past decade, the field of nanowire research has advanced to the stage that materials of essentially any composition can be made into nanowires with desired sizes and aspect ratio. Consequently, there are now a host of nanowire materials that can be used as stable templates. The conformal coating of a high aspect ratio nanostructure is made possible by exploring several state-of-the-art vapor phase deposition techniques, including MOCVD, atomic layer deposition (ALD), pulsed laser deposition, or sputtering. The availability of these advanced deposition techniques allows the conformal coating of the sheath materials of almost any compositions, such as nitrides, oxides, metals, carbon, and even polymers, although lattice match is required for the making of single-crystalline nanotubes. Figure 2 shows a collection of TEM and SEM images of a variety of inorganic nanotubes prepared with this approach. This nanotube fabrication technique largely resembles the lost-wax process, a sculpture technique invented thousands of years ago. In the lost-wax technique, still used by many bronze sculptors today, a wax template is created and then coated with wet clay. After the clay hardens, the wax template is melted away, leaving behind a shell into which the molten bronze is poured.

We have applied this nanowire-templating approach toward the rational synthesis of many other nanotubular materials. For example, by using ZnO nanowires as

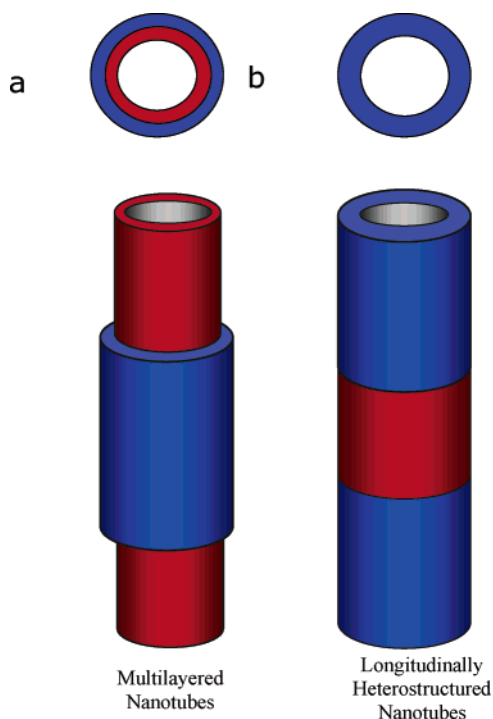


**FIGURE 3.** Schematic drawings (cross-sectional and perspective view) of several possible complex nanotube structures: (a) multilayered nanotubes; (b) longitudinal junctioned nanotubes.

templates, we have made single-crystalline  $\text{In}_x\text{Ga}_{1-x}\text{N}$ , GaN/Mn nanotubes (Figure 2a) via MOCVD deposition, branched silica nanotubes from ZnO tetrapods (Figure 2b), and polycrystalline or amorphous  $\text{TiO}_2$  nanotubes via atomic-layer deposition of  $\text{TiO}_2$  (Figure 2c). In all of these cases, the inner ZnO nanowire is preferentially etched using acidic solutions. Additionally, we have chemically bound polymer initiators to both ZnO nanowires and partially oxidized Si nanowires to produce conformal coatings of numerous polymers, including poly(methyl methacrylate) polymer, which result in multishelled nanotubular materials upon subsequent etching of the inner nanowire. Finally, there have been numerous reports on the creation of other nanotubular materials using similar processes. The compositions of the inorganic nanotubes now include metal, oxide, and group IV, II–VI, and III–V semiconductors.<sup>13–18</sup> This nanowire-templating process is apparently a fairly universal process and can be used to produce a wide array of nanotubular materials.

With some simple extension, this process can be readily adapted for the making of nanotubes with much higher complexity. Multilayered nanotubes (Figure 3a) can be made through sequential multistep conformal coating. For example, through multiple steps of sputtering, we were able to make multilayered Si/SiO<sub>2</sub> nanotubes (Figure 2d) using ZnO as templates. These multilayered nanotubes could have unique optical waveguiding properties. Similarly, nanotubes with longitudinal heterojunctions (Figure 3b) can be envisioned through properly designed conformal coating procedures.

Alternatively, the sheath materials can be directly produced on the surface of the nanowire templates through surface reactions such as oxidations. In our lab,

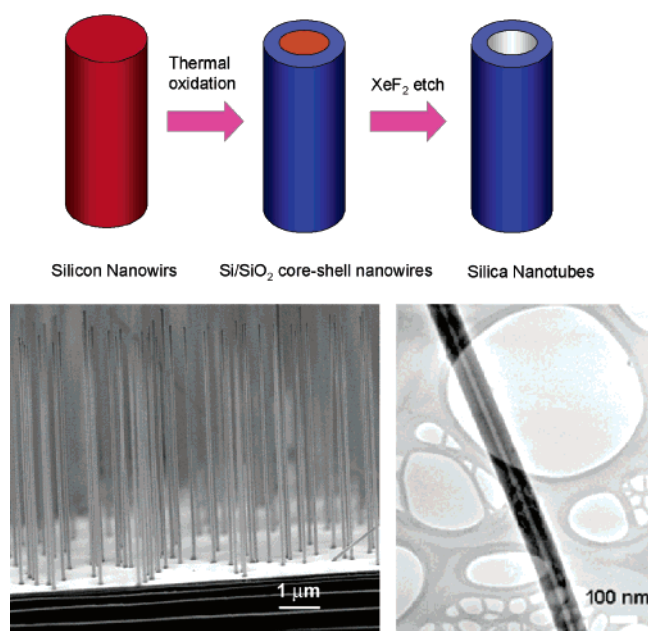


**FIGURE 4.** Oxidation–etching approach to synthesize vertical silica nanotube arrays from silicon nanowire templates. The bottom panels show the scanning electron micrographs of the as-grown silicon nanowire array and the transmission electron image of a representative silica nanotube.

amorphous SiO<sub>2</sub> nanotubes were produced by the high-temperature thermal oxidation of silicon nanowires.<sup>19</sup> As schematically shown in Figure 4a, silicon nanowires were thermally oxidized to form Si/SiO<sub>2</sub> core/shell wires. Then XeF<sub>2</sub> was used to selectively etch out the remaining silicon cores to yield hollow tubular structures. In Figure 4, the SEM and TEM images show the silicon nanowire templates and the silica nanotube after the oxidation–etching processes, respectively. The resultant nanotubes formed have inner diameters that can be controlled by adjusting the thermal oxidation temperature and time. These nanotubes generally have inner diameter of 5–20 nm. With further optimization and control of the oxidation and etching process, we should be able to form nanotubes with inner diameters of less than 5 nm. One major advantage of these nanotubes is that our silica walls are much more condensed than those prepared using anodic alumina templates, because silica grown via low-temperature solution-based techniques tend to have higher porosities. In addition, the inner surfaces of our silica nanotubes are very smooth, and their sizes can be tuned from 1 to 100 nm, which is ideally suited for our nanofluidic studies. In addition, the silica surface chemistry is readily available for covalent attachment of desired receptors on the inner wall of the nanocapillary.

In principle, a similar approach can be used to produce nanotubes of other compositions, such as sulfide, selenide, nitride, and carbide. A one-dimensional Kirkendall effect<sup>20</sup> can be used here to produce hollow nanotubes of various compositions by exploring the different diffusion characteristics of the individual elements. For example, one can start with silver wires coated with a thin sheath of selenium; a thermal treatment may create Ag<sub>2</sub>Se nanotubes.

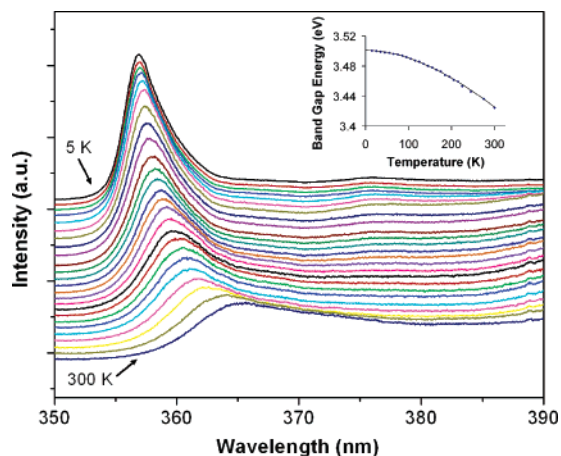


**FIGURE 5.** Temperature-dependent photoluminescence spectra of an individual GaN nanotube. The spectra collected from top to bottom correspond to measurements collected at different temperatures between 5 and 300 K. The inset is the fit of the band gap emission vs temperature to  $\alpha = 0.95$  meV/K and  $\beta = 830$  K.

### Photoluminescence and Electron Transport in GaN Nanotubes

Gallium nitride is a wide band gap semiconductor ( $E_g = 3.47$  eV), which has recently garnered much attention for numerous applications including high-intensity, efficient LEDs.<sup>21,22</sup> Deep level defects are known to plague GaN thin film materials and are generally responsible for the presence of broad yellow to red band emission in photoluminescence measurements of GaN thin films.<sup>23</sup> The actual chemical nature of these defects is still hotly disputed and has been attributed to both misfit dislocations and point source impurities such as oxygen and carbon. Nevertheless, the presence of these deep level defects in our nanotubes would be detrimental for applying these nanotubes in optical sensing applications. Through optimization of the MOCVD synthesis conditions, we have been able to create GaN nanotubes that lack any broad band emission and have an optical photoluminescence that is comparable to the highest quality GaN thin films.

Figure 5 is a temperature-dependent series of photoluminescence (PL) spectra of an individual nanotube with  $\sim 15$  nm shell thicknesses. These spectra were collected from 6.2 to 300 K. The band gap peak at 356 nm at low temperatures corresponds to the band gap emission of GaN and is comparable to the bulk value. The variation of the band gap emission energy with respect to temperature is plotted in the inset. By empirically fitting this plot to the Varshni expression,<sup>24</sup> we obtain  $\alpha$  and  $\beta$  parameters of  $\alpha = 0.95$  meV/K and  $\beta = 830$  K, which are comparable to the values reported for high-quality low-defect thin films.<sup>25,26</sup> These PL studies indicate that we have an ideal stress-free semiconductor system. In addition, electron transport measurements (Figure 6) indicate that the resistances of these nanotubes are on the order of 10 M $\Omega$  at room temperature and increase with decreasing temperature. The conductive semiconductor nature of these GaN nanotubes opens up the possibility of their use for simultaneous resistive, optical, and ionic sensing.<sup>27,28</sup>

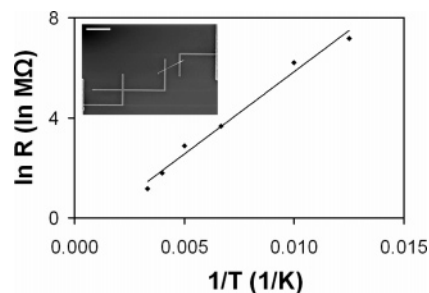


**FIGURE 6.** Electrical properties of a single-crystalline GaN nanotube. The dependence on resistance ( $R$ ) for a typical GaN nanotube two-probe device shows semiconducting behavior. The typical room-temperature resistivity is about 100  $\Omega$  cm. The inset shows an SEM image of a two-probe device (scale bar = 10  $\mu$ m).

### Emergence of Unipolar Ionic Environment: Nanofluidics vs Microfluidics

At first glimpse of these inorganic nanotubes, one might consider them as nanoscale test tubes or pipes for liquid/solution processing. Indeed, early synthetic efforts in making silica nanotubular membranes using porous alumina templates had already inspired people to investigate their liquid transport characteristics.<sup>29</sup> Voltage-controlled ionic flux selection and molecular separation have been demonstrated using the nanotubule membranes.<sup>30–32</sup> Silica nanotube suspensions have also been employed as nanocontainers for “smart” extraction and gene delivery.<sup>33,34</sup>

The nanotubular materials that can be used in nanofluidic experiments must satisfy several criteria. These nanotubes must (1) have a well-controlled inner diameter that can range from 1 to 100 nm, (2) be structurally robust and, ideally, continuous and seamless, (3) be easily functionalized on inner and outer surfaces, (4) be chemically stable, and (5) have a variable length. Carbon nanotubes and other tubular structures (BN, sulfides) may not be suitable for such a purpose because of not satisfying one or more of these criteria. Recently, the Martin group has been successful in employing tubular structures prepared via a solution templating process (porous alumina as templates) for biological separation purposes.<sup>35</sup> However, the robustness and integrity of the nanotubes prepared this way are less than ideal, and their inner diameters are generally 50 nm or above.

Now let us consider the nanotube–electrolyte interface. When an electrolyte solution is confined within a silica nanotube with negative surface charges, counterions accumulate near a charged surface and co-ions are electrostatically repelled.<sup>36</sup> Due to this counterion shield, the electric potential decays to its bulk value over a characteristic length known as the Debye length. The Debye length,  $\lambda_D$ , decreases as the ion concentration,  $n$ , increases,  $\lambda_D \propto n^{-1/2}$ , and is typically 1–100 nm for aqueous solutions. In micrometer-sized channels, the Debye length is usually much smaller than the channel dimensions, and the bulk of the solution is shielded from the surface charge. Therefore, although interfacial effects such as electroosmotic flow can be controlled using field-effect and surface modification in microchannels,<sup>37</sup> direct elec-

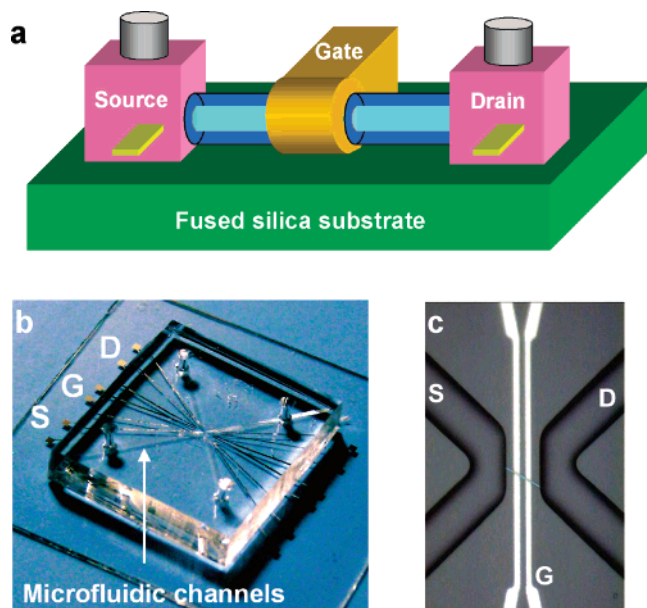


**FIGURE 7.** Single nanotube based metal–oxide solution field effect transistors (MOSolFETs): (a) schematic structure of a MOSolFET; (b) a fully packaged nanotube nanofluidic transistor; (c) a light microscopy image showing the device structure—source (S) and drain (D) microfluidic channels, the metallic gate (G), and the single silica nanotube.

trostatic manipulation of ions across the microchannel is not possible. However, nanometer-sized channels, which have one dimension comparable to or smaller than the Debye length, possess an electrostatic potential that remains nonzero even in the center of the nanotube. Thus, the solution becomes unipolar since the cations are more concentrated than the anions.

We found that the ionic conductance through a nanotube filled with low-concentration KCl solution significantly deviates from bulk behavior once the KCl concentration is lower than 10 mM.<sup>38</sup> This is a clear indication of the emergence of a unipolar transport that is not dependent on bulk KCl concentration but rather is controlled by surface charges. Unipolar transport is unique only in nanofluidic channels and is absent in microfluidic systems due to strong Debye screening in aqueous solution. Furthermore, in nanochannels, electrostatic fields can penetrate throughout the channel, enabling direct control of ionic/molecular transport by adjusting surface potential or charges in such nanochannels. An early work over a decade ago investigated this phenomenon in glycerol-filled nanochannels.<sup>39</sup> This gate control represents one of the major advantages over much of the work on nanopores.<sup>40,41</sup>

## Metal–Oxide Solution Field Effect Transistors (MOSolFETs)

A comparison with typical unipolar electronic devices, for example, metal–oxide semiconductor (MOS) systems, leads to the concept that a gate voltage may be employed to modulate the ionic concentration in nanotubes. Figure 7a is the schematic design of single nanotube metal–oxide solution field effect transistors (MOSolFETs).<sup>36</sup>

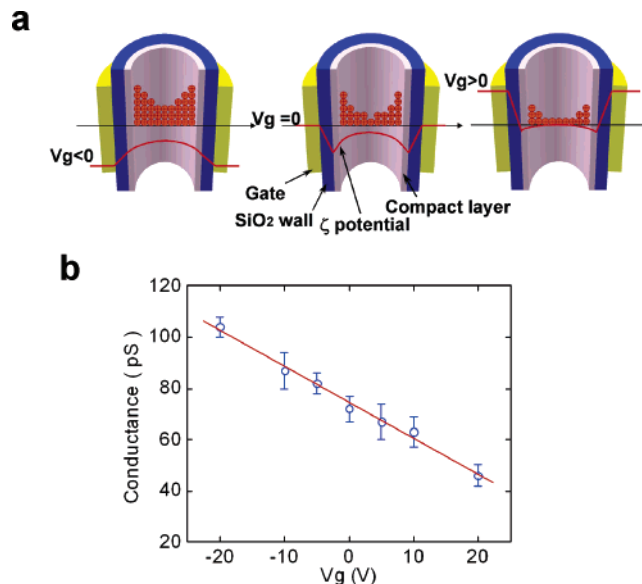


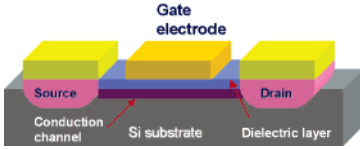
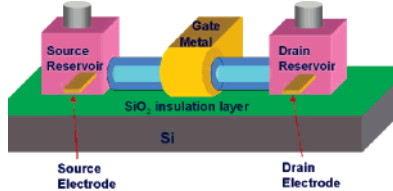
**FIGURE 8.** Field effect modulation of ionic conductance: (a) schematic mechanism of field effect modulation—red lines showing the potential diagram across nanotubes at various gate voltages and dots qualitatively representing the ionic density and distribution; (b) the transfer characteristics (differential conductance vs gate voltage) of a nanotube nanofluidic transistor (adapted from ref 42).

Here, we have integrated our silica nanotubes, which have high aspect ratio, excellent uniformity, and surface smoothness, into nanofluidic transistors by interfacing with two microfluidic channels. Figure 7b shows a fully packaged silica nanotube nanofluidic device with a polydimethylsiloxane (PDMS) cover in which access holes are drilled prior to bonding. The MOSolFET device (Figure 7c) includes source (S)/drain (D) microfluidic channels and the metallic gate electrodes (G).

Figure 8b shows the ionic conductance through a silica nanotube with potassium chloride solution ( $\leq 1$  mM) under different gate voltages ( $V_g$ ). This device clearly exhibits p-type transistor behavior indicating that cations ( $K^+$ ) are the major electronic carriers through the silica nanotubes. Negative  $V_g$  enhances carrier concentration, while positive  $V_g$  depletes carriers. The conductance values were derived from the slopes of steady-state  $I/V$  curves to avoid zero shift and nonequilibrium effects.<sup>42</sup>

These results demonstrate that, analogous to the field effect modulation of the band diagram in metal–oxide semiconductor (MOS) systems, the gate voltage can tune the electrostatic potential of the solution inside the nanotubes. Figure 8a is an illustration of the electrostatic potential diagram for our MOSolFET device. At the  $SiO_2$ /liquid interface, an electrical double layer (EDL) forms to screen the surface potential. The EDL consists of two layers, the inner compact layer (Stern layer) and the outer diffuse layer. In a fluid medium sufficiently larger than the thickness of the diffuse layer, the electrostatic potential decays from the effective surface potential ( $\zeta$  potential) to zero. When the solution is in a confined geometry, for example, when the nanotube radius is comparable to or smaller than the diffuse layer, the electrical potential in

**Table 1. Comparison between a Metal–Oxide Semiconductor Field Effect Transistor (MOSFET) and a MOSolFET**

	MOSFET	MOSolFET
device structure		
carrier	electron/hole	anion/cation
polarity	unipolar	unipolar/bipolar
mobility	high	low
carrier concentration	doping level	surface charge density
conduction channel	2D electron/hole conduction layer	Debye layer (1–100 nm thick)
applications	control of electrical conductance	control of ionic/molecular environment or transport.

the center of nanotube remains nonzero. Because  $\text{SiO}_2$  surfaces are typically negatively charged due to the presence of hydroxyl and  $\text{Si-O}^-$  groups, cations act as the majority carriers and the resulting transistors are *p*-FETs. Negative  $V_g$  shifts down the overall potential and leads to accumulation of cations, thus increasing the electrical conductance. Positive  $V_g$  depletes cations and decreases electrical conductance. This simple scheme qualitatively explains how field effect control works in nanofluidic systems. This first realization of a MOSolFET device establishes the ability to use electric fields to control the transport of charged species on the nanoscale and suggests the possibility of utilizing this ability in various fluidic applications, such as in chemical logic devices or for the controlled step-by-step delivery of chemical reactants into one-pot microreactors.

### Doping Control in Nanotube Nanofluidic Transistors

Analogous to MOS transistors, it is desirable to tune the “doping level” and thereby change the inherent carrier concentrations or type. We have shown that the inherent carrier concentration in our nanofluidic transistors can be controlled by adjusting the inner surface potential and charge density via the application of a gate voltage. In this regard, changing the native surface charge density via chemical modification is expected to have similar consequences in nanofluidic transistors as changing the dopant concentration of the semiconductors in MOSFETs (Table 1). A reduced doping level is generally associated with a more pronounced field effect modulation in semiconductors.<sup>43</sup> We now turn to the impact of surface modification on the field effect for our metal–oxide solution field effect transistors (MOSolFETs).

Aminosilane chemistry has been used to modify inner surfaces of silica nanotubes to change the surface potential and charge density or even switch channel polarity. Right before PDMS cover bonding, the nanotube was treated with 3-amino-propyl triethoxyl silane (APTES) (Figure 9a), while the transistor characteristics were monitored over the surface functionalization duration. It was found that 1 day of APTES functionalization did not change polarity (still *p*-type behavior) but led to a greatly reduced ionic

conductance and a more pronounced gating effect as shown in Figure 9b. The ionic conductance exhibits a much more profound field effect modulation.

The polarity of the nanotube ionic transistors can be completely reversed after a prolonged surface modification. Four days of APTES treatment converted as-made *p*-FETs into *n*-FETs (Figure 9c). In this case, the ionic conductance increased with increasing  $V_g$  for the entire experimental range of  $V_g$ .

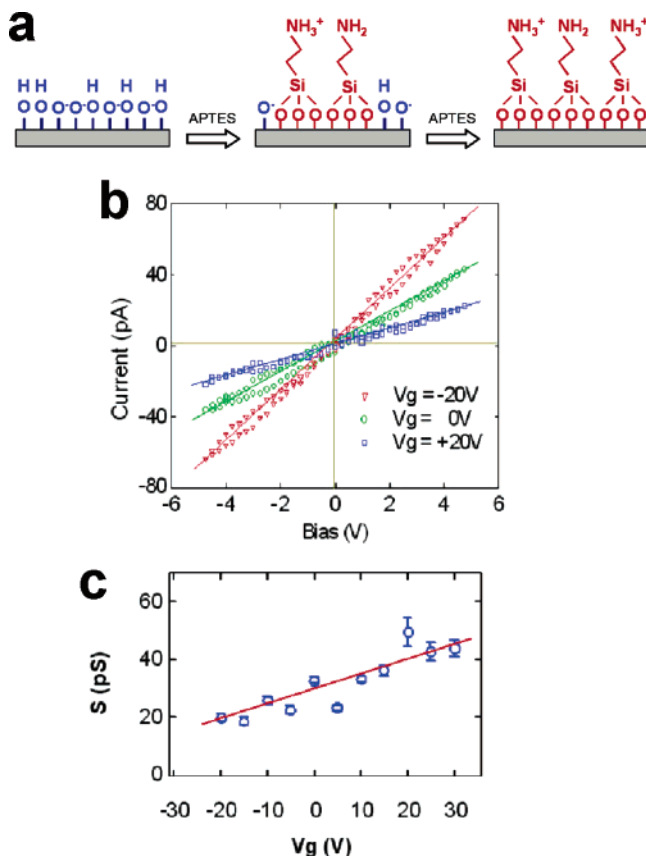


**FIGURE 9.** “Doping” control and polarity switching: (a) scheme of surface modification with APTES; (b) selected  $I/V$  curves for the nanotube nanofluidic transistor after 1 day of APTES functionalization, showing enhanced *p*-type field effect behavior at a lower surface charge density; (c) differential conductance vs gate voltages ( $V_g$ ) for the nanofluidic transistors after 4 days of APTES treatment, showing a polarity change to an *n*-type FET (adapted from ref 42).

## Single Molecule Sensing using Nanotube Nanofluidics: Interplay of Charge Effect and Geometry Effect

Sensors utilizing novel nanostructured materials and new mechanisms will have a significant impact on a broad range of applications relating to national security, health care, the environment, energy, food safety, and manufacturing. Emerging micro- and nanotechnologies can decrease the size, weight, and cost of sensors and sensor arrays by orders of magnitude while simultaneously increasing their spatial and temporal resolution and accuracy. Over the years, various molecular detection techniques have been developed and validated for their chemical/biological sensing, diagnostic, and prognostic utility. For most, efficiency is a result of a tradeoff between sensitivity, specificity, ease of operation, cost, speed, and frequency of false alarms. Novel functional materials such as quantum dots, photonic crystals, nanowires, carbon nanotubes, porous membranes, porous silicon, and sol-gel matrixes incorporating biomolecules have been used as sensing elements with various possible detection mechanisms.

Because of their similar dimensions, inorganic nanotube nanofluidic transistors can be employed for single biomolecule sensing using a detection scheme based on monitoring ionic current through a single nanotube. Once a biomolecule, such as  $\lambda$ -phage DNA, drifts into the nanotube, their interaction will change the ionic current and give rise to a transient signal for the DNA translocation event. Based on this electrical detection scheme, channel protein nanopores have been utilized as single-molecule sensors based on ionic current blockage<sup>40</sup> and have exhibited promise for ultrafast DNA sequencing.<sup>41,44</sup> Artificial nanopores have also been used for single-molecule sensing and configurational studies.<sup>45–49</sup> Our inorganic nanotubes have quite unique dimensions with nanometer scale inner diameter and ultrahigh aspect ratio (which enables field effect control).

In our experiments,<sup>50</sup> the translocation of single  $\lambda$ -DNA molecules through the nanotubes was studied at two different ionic concentrations, 2 and 0.5 M KCl. When the microfluidic channels were first filled with 2 M KCl solution and the current through the nanotube was measured with the application of electrical bias, the ionic conductance exhibited a stable baseline with  $\sim 15$ – $20$  pA fluctuations prior to loading DNA molecules. When  $\lambda$ -DNA in 2 M KCl buffer solution was introduced to the negatively biased microchannel (with the other microchannel filled with 2 M KCl buffer only), the ionic current exhibited many current drops corresponding to passage of individual  $\lambda$ -DNA molecules (Figure 10a). These current drop events may be attributed to the volume exclusion of conducting ions, which leads to a transient ionic current blockage. The typical current change is 10–40 pA. The typical duration of the translocation events is 4–10 ms with a small number of events lasting up to 20 ms. The overall distribution is quite narrow with mean current change and translocation time of 23 pA and 7.5 ms

respectively (Figure 10b), suggesting that a majority of the events are identical and correspond to single molecule translocation events. Interestingly, when the same experiment was conducted in a lower concentration of KCl solution (0.5 M), a distinctly different phenomenon was observed. Instead of decrease in current, the ionic current increased during the translocation of  $\lambda$ -DNA molecules (Figure 10c,d). Statistics of current change and duration time shows a much broader distribution.

The observed results can be explained by a simplified model that considers the charge and volume of the DNA molecule (i.e., charge effect vs geometry effect). For a biomolecule with charge  $q$  and volume  $V$  present in a solution with ionic concentration  $c$  in the nanotube, the number of charges on the biomolecule is  $q/e$ , where  $e$  is the charge of an electron. When this molecule is introduced into the nanotube, it will attract counterions that neutralize its surface charge. Therefore, the excess number of mobile carrier ions introduced into the nanotube due to the biomolecule is given approximately by

$$n_{\text{charge}} = fq/e \quad (1)$$

where  $f$  is the ratio of the effective number of excess mobile ions to the number of charges on the biomolecule. On the other hand, the number of ions excluded by the biomolecule is simply given by

$$n_{\text{volume}} = cV \quad (2)$$

Biomolecule charge and volume have opposite effects on nanotube conductance: excess charge increases the number of conducting ions in the nanotube, whereas volume exclusion of ions decreases the number of conducting ions. These relations suggest a critical ionic concentration,  $c_{\text{critical}}$ , at which the two competing effects balance, that is,  $n_{\text{charge}} = n_{\text{volume}}$ . The critical concentration is given by

$$c_{\text{critical}} = fq/(eV) \quad (3)$$

The critical concentration is thus uniquely determined by the effective charge density and volume of the biomolecule. Below the critical concentration, the charge effect is dominant, resulting in an increase in ionic conductance of the nanotube in the presence of the biomolecule. Above the critical concentration, the volume effect is dominant, resulting in a decrease in ionic conductance.

In the case of DNA in the nanotube, both the silica tube walls and the DNA molecule are negatively charged. We applied the above simple model to calculate the expected critical concentration for the  $\lambda$ -DNA molecule. This calculation gives a critical concentration of 0.78 M. The calculated critical concentration is in good agreement with the current increase observed at 0.5 M and current decrease observed at 2 M KCl. While the model proposed here qualitatively explains our experimental observation, we note that this is perhaps an oversimplified account of the highly complex DNA transport process within nanotubes. Nonetheless, we show that when biomolecules are present inside nanofluidic tubes, the ionic conductance reflects a rich interplay between the competing effects of

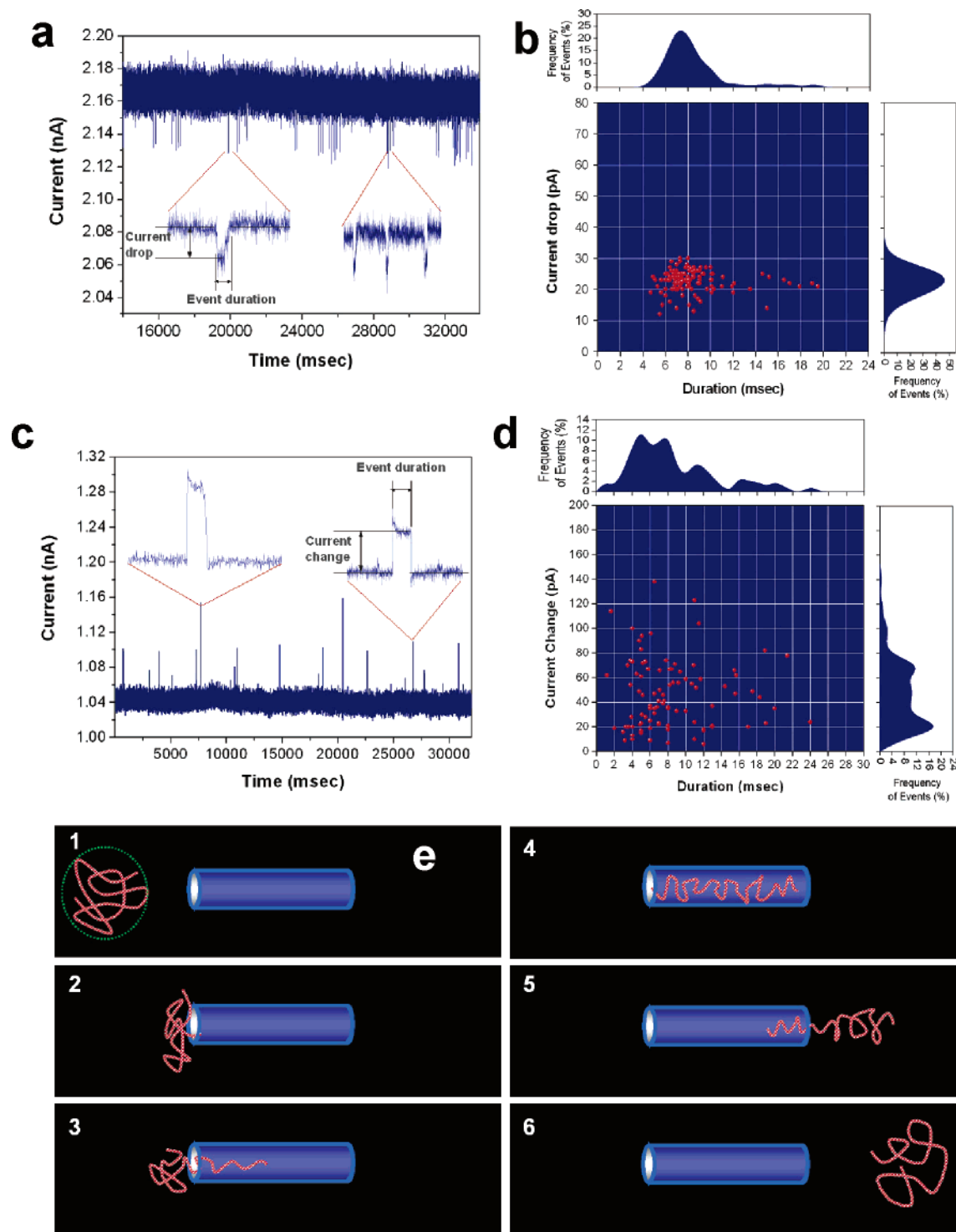


**FIGURE 10.** Single DNA molecule detection in nanotubes. Panels a and b are ionic current signals for  $\lambda$ -DNA translocations at  $[KCl] = 2\text{ M}$  and the statistics of current change and duration time. Panels c and d are data for experiments carried out at  $[KCl] = 0.5\text{ M}$  (adapted from ref 50). Panel e shows a schematic illustration of DNA translocation through a long nanotube, in which a complex DNA conformational evolution is involved.

biomolecule charge and size. It is worth noting that the charge-to-mass ratio of biomolecules is a key parameter in mass spectrometry, which is now widely used to characterize and identify biomolecules. In a similar manner, the charge-to-volume ratio extracted from nanofluidic ion conductance measurements could potentially become a method of characterizing biomolecules as well. In contrast to mass spectrometry, nanofluidics could enable

single-molecule sensitivity in subfemtoliter volumes of aqueous environment, as demonstrated here.

The exact nature of the DNA or other biomolecule transport within nanotubes (Figure 10e) still requires a significant amount of additional theoretical and experimental investigation. The entropic barrier mediated translocation will lead to a different conformational evolution, which could be reflected in the fine structure of every



ionic current peak. Interestingly, all the signal peaks exhibit similar shapes for either current blockade or current increase. We conjecture that the evolution of the ionic current may be related to the evolution of the chain conformations during the translocation of DNA as shown in Figure 10e. The inorganic nanotube nanofluidic device lengthens the single molecule transport events greatly in time scale compared to the nanopore devices.<sup>40,41</sup> In addition, the duration, the current change, and the current decay characteristics measured at different ionic concentrations and biases would provide useful information on biomolecules within a confined geometry. Therefore, these nanotube devices represent a novel platform for studying single-molecule behavior.

## Conclusion and Outlook

The inorganic nanotubes introduced here possess several characteristics that are beneficial for their application in optoelectronics and nanofluidics. They feature controllable inner diameter from 1 to 100 nm, structural robustness, easy functionalization of inner and outer surfaces, chemical stability, and tunable compositions and aspect ratio. In particular, the ability to spatially and temporally tune the ionic and electrostatic environment makes nanotube-based nanofluidic transistors a unique tool for biological and chemical analyses in femtoliter volumes. The single nanotube transistors have the ability to manipulate and sense extremely small amounts of charged species or even single biomolecules. Similar to metal-oxide semiconductor field effect transistors, the nanofluidic transistor has the potential to form the building blocks of integrated nanofluidic circuits for manipulating biomolecules with single-molecule precision and control.

In addition, previously, semiconductor thin films have been extensively studied for their chemical and biological field effect transistor applications. Our semiconductor nanotubes (GaN) have the following characteristics that would be ideal for such applications: mechanically robust, electrically and optically active, and extremely high internal and external surfaces. It is fairly common that different molecular species on the surface of the nanotubes will induce different surface charge/potentials, and in many cases, electron transfer would occur. Both factors would readily induce the conductivity change within the semiconductor GaN nanotubes. Both the internal and external surface can be used as active probe areas for sensing purposes, which would dramatically increase the sensitivity. Obviously we could also measure the ionic current simultaneously if needed. The simultaneous feedback of multiple electrical signals (as well as single molecular optical signal within the confined nanotube geometry) would allow us to perform chemical and biological sensing with high sensitivity and specificity and much fewer false alarms. Overall this new class of one-dimensional nanostructures is posed to have a great impact not only in the traditional sectors of nanoscience research including photonics and electronics, but also in

opening up a new research paradigm in the area of nanofluidics at the bio-nano interface.

*This work is supported by National Science Foundation, National Institutes of Health, and Office of Basic Science, Department of Energy. We are very grateful to our co-workers on the nanofluidic project, Prof. Arun Majumdar and Rohit Karnik. We thank the National Center for Electron Microscopy for the use of their facilities.*

## References

- (1) Iijima, S. Helical Microtubules of Graphitic Carbon. *Nature* **1991**, *354*, 56–58.
- (2) Law, M.; Goldberger, J.; Yang, P. D. Semiconductor nanowires and nanotubes. *Annu. Rev. Mater. Res.* **2004**, *34*, 83–122.
- (3) Rapoport, L.; Fleischer, N.; Tenne, R. Applications of WS<sub>2</sub> (MoS<sub>2</sub>) inorganic nanotubes and fullerene-like nanoparticles for solid lubrication and for structural nanocomposites. *J. Mater. Chem.* **2005**, *15*, 1782–1788.
- (4) Tenne, R. Inorganic nanoclusters with fullerene-like structure and nanotubes. *Prog. Inorg. Chem.* **2001**, *50*, 269–315.
- (5) Tenne, R.; Zettl, A. K. Nanotubes from inorganic materials. *Top. Appl. Phys.* **2001**, *80*, 81–112.
- (6) Li, Y. D.; Wang, J. W.; Deng, Z. X.; Wu, Y. Y.; Sun, X. M.; Yu, D. P.; Yang, P. D. Bismuth nanotubes: A rational low-temperature synthetic route. *J. Am. Chem. Soc.* **2001**, *123*, 9904–9905.
- (7) Patzke, G. R.; Krumeich, F.; Nesper, R. Oxidic nanotubes and nanorods – Anisotropic modules for a future nanotechnology. *Angew. Chem., Int. Ed.* **2002**, *41*, 2446–2461.
- (8) Xiong, Y. J.; Mayers, B. T.; Xia, Y. N. Some recent developments in the chemical synthesis of inorganic nanotubes. *Chem. Commun.* **2005**, 5013–5022.
- (9) Martin, C. R. Nanomaterials – a Membrane-Based Synthetic Approach. *Science* **1994**, *266*, 1961–1966.
- (10) Ajayan, P. M.; Stephan, O.; Redlich, P.; Colliex, C. Carbon Nanotubes as Removable Templates for Metal-Oxide Nanocomposites and Nanostructures. *Nature (London)* **1995**, *375*, 564–567.
- (11) Kondo, Y.; Takayanagi, K. Synthesis and characterization of helical multi-shell gold nanowires. *Science* **2000**, *289*, 606–608.
- (12) Goldberger, J.; He, R. R.; Zhang, Y. F.; Lee, S. W.; Yan, H. Q.; Choi, H. J.; Yang, P. D. Single-crystal gallium nitride nanotubes. *Nature (London)* **2003**, *422*, 599–602.
- (13) Li, Y. B.; Bando, Y.; Golberg, D.; Liu, Z. W. Ga-filled single-crystalline MgO nanotube: Wide-temperature range nanothermometer. *Appl. Phys. Lett.* **2003**, *83*, 999–1001.
- (14) Sun, Y. G.; Xia, Y. N. Multiple-walled nanotubes made of metals. *Adv. Mater.* **2004**, *16*, 264–268.
- (15) Hu, J. Q.; Bando, Y.; Liu, Z. W.; Zhan, J. H.; Golberg, D.; Sekiguchi, T. Synthesis of crystalline silicon tubular nanostructures with ZnS nanowires as removable templates. *Angew. Chem., Int. Ed.* **2004**, *43*, 63–66.
- (16) Hu, J. Q.; Bando, Y.; Zhan, J. H.; Golberg, D. Sn-filled single-crystalline Wurtzite-type ZnS nanotubes. *Angew. Chem., Int. Ed.* **2004**, *43*, 4606–4609.
- (17) Yin, L. W.; Bando, Y.; Zhu, Y. C.; Li, M. S.; Tang, C. C.; Golberg, D. Single-crystalline AlN nanotubes with carbon-layer coatings on the outer and inner surfaces via a multiwalled-carbon-nanotube-template-induced route. *Adv. Mater.* **2005**, *17*, 213–217.
- (18) Li, Y. B.; Bando, Y.; Golberg, D. Indium-assisted growth of aligned ultra-long silica nanotubes. *Adv. Mater.* **2004**, *16*, 37–40.
- (19) Fan, R.; Wu, Y. Y.; Li, D. Y.; Yue, M.; Majumdar, A.; Yang, P. D. Fabrication of silica nanotube arrays from vertical silicon nanowire templates. *J. Am. Chem. Soc.* **2003**, *125*, 5254–5255.
- (20) Yin, Y. D.; Rioux, R. M.; Erdonmez, C. K.; Hughes, S.; Somorjai, G. A.; Alivisatos, A. P. Formation of hollow nanocrystals through the nanoscale Kirkendall Effect. *Science* **2004**, *304*, 711–714.
- (21) Nakamura, S. UV/blue/green InGaN-based LEDs and laser diodes grown on epitaxially laterally overgrown GaN. *IEICE Trans. Electron.* **2000**, *E83C*, 529–535.
- (22) Nakamura, S.; Mukai, T.; Senoh, M. High-Power GaN P–N Junction Blue-Light-Emitting Diodes. *Jpn. J. Appl. Phys., Part 2* **1991**, *30*, L1998–L2001.
- (23) Reshchikov, M. A.; Morkoc, H. Luminescence properties of defects in GaN. *J. Appl. Phys.* **2005**, *97*.
- (24) Varshni, Y. P. Temperature Dependence of Energy Gap in Semiconductors. *Physica* **1967**, *34*, 149–154.
- (25) Passler, R. Dispersion-related assessments of temperature dependences for the fundamental band gap of hexagonal GaN. *J. Appl. Phys.* **2001**, *90*, 3956–3964.

- (26) Fischer, A. J.; Shan, W.; Song, J. J.; Chang, Y. C.; Horning, R.; Goldenberg, B. Temperature-dependent absorption measurements of excitons in GaN epilayers. *Appl. Phys. Lett.* **1997**, *71*, 1981–1983.
- (27) Kim, J. R.; So, H. M.; Park, J. W.; Kim, J. J.; Kim, J.; Lee, C. J.; Lyu, S. C. Electrical transport properties of individual gallium nitride nanowires synthesized by chemical-vapor-deposition. *Appl. Phys. Lett.* **2002**, *80*, 3548–3550.
- (28) Huang, Y.; Duan, X. F.; Cui, Y.; Lieber, C. M. Gallium nitride nanowire nanodevices. *Nano Lett.* **2002**, *2*, 101–104.
- (29) Kuo, T. C.; Sloan, L. A.; Sweedler, J. V.; Bohn, P. W. Manipulating molecular transport through nanoporous membranes by control of electrokinetic flow: Effect of surface charge density and Debye length. *Langmuir* **2001**, *17*, 6298–6303.
- (30) Lee, S. B.; Martin, C. R. Electromodulated molecular transport in gold-nanotube membranes. *J. Am. Chem. Soc.* **2002**, *124*, 11850–11851.
- (31) Nishizawa, M.; Menon, V. P.; Martin, C. R. Metal Nanotubule Membranes with Electrochemically Switchable Ion-Transport Selectivity. *Science* **1995**, *268*, 700–702.
- (32) Kang, M. S.; Martin, C. R. Investigations of potential-dependent fluxes of ionic permeates in gold nanotubule membranes prepared via the template method. *Langmuir* **2001**, *17*, 2753–2759.
- (33) Mitchell, D. T.; Lee, S. B.; Trofin, L.; Li, N. C.; Nevanen, T. K.; Soderlund, H.; Martin, C. R. Smart nanotubes for bioseparations and biocatalysis. *J. Am. Chem. Soc.* **2002**, *124*, 11864–11865.
- (34) Chen, C. C.; Liu, Y. C.; Wu, C. H.; Yeh, C. C.; Su, M. T.; Wu, Y. C. Preparation of fluorescent silica nanotubes and their application in gene delivery. *Adv. Mater.* **2005**, *17*, 404–407.
- (35) Lee, S. B.; Mitchell, D. T.; Trofin, L.; Nevanen, T. K.; Soderlund, H.; Martin, C. R. Antibody-based bio-nanotube membranes for enantiomeric drug separations. *Science* **2002**, *296*, 2198–2200.
- (36) Daiguji, H.; Yang, P. D.; Majumdar, A. Ion transport in nanofluidic channels. *Nano Lett.* **2004**, *4*, 137–142.
- (37) Schasfoort, R. B. M.; Schlautmann, S.; Hendrikse, L.; van den Berg, A. Field-effect flow control for microfabricated fluidic networks. *Science* **1999**, *286*, 942–945.
- (38) Karnik, R.; Fan, R.; Yue, M.; Li, D. Y.; Yang, P. D.; Majumdar, A. Electrostatic control of ions and molecules in nanofluidic transistors. *Nano Lett.* **2005**, *5*, 943–948.
- (39) Gajar, S. A.; Geis, M. W. An Ionic Liquid-Channel Field-Effect Transistor. *J. Electrochem. Soc.* **1992**, *139*, 2833–2840.
- (40) Kasianowicz, J. J.; Brandin, E.; Branton, D.; Deamer, D. W. Characterization of individual polynucleotide molecules using a membrane channel. *Proc. Natl. Acad. Sci. U.S.A.* **1996**, *93*, 13770–13773.
- (41) Deamer, D. W.; Akeson, M. Nanopores and nucleic acids: prospects for ultrarapid sequencing. *Trends Biotechnol.* **2000**, *18*, 147–151.
- (42) Fan, R.; Yue, M.; Karnik, R.; Majumdar, A.; Yang, P. D. Polarity switching and transient responses in single nanotube nanofluidic transistors. *Phys. Rev. Lett.* **2005**, *95*, No. 086607.
- (43) Cui, Y.; Duan, X. F.; Hu, J. T.; Lieber, C. M. Doping and electrical transport in silicon nanowires. *J. Phys. Chem. B* **2000**, *104*, 5213–5216.
- (44) Howorka, S.; Cheley, S.; Bayley, H. Sequence-specific detection of individual DNA strands using engineered nanopores. *Nat. Biotechnol.* **2001**, *19*, 636–639.
- (45) Li, J. L.; Gershow, M.; Stein, D.; Brandin, E.; Golovchenko, J. A. DNA molecules and configurations in a solid-state nanopore microscope. *Nat. Mater.* **2003**, *2*, 611–615.
- (46) Saleh, O. A.; Sohn, L. L. An artificial nanopore for molecular sensing. *Nano Lett.* **2003**, *3*, 37–38.
- (47) Storm, A. J.; Storm, C.; Chen, J. H.; Zandbergen, H.; Joanny, J. F.; Dekker, C. Fast DNA translocation through a solid-state nanopore. *Nano Lett.* **2005**, *5*, 1193–1197.
- (48) Mara, A.; Siwy, Z.; Trautmann, C.; Wan, J.; Kamme, F. An asymmetric polymer nanopore for single molecule detection. *Nano Lett.* **2004**, *4*, 497–501.
- (49) Siwy, Z.; Fulinski, A. Fabrication of a synthetic nanopore ion pump. *Phys. Rev. Lett.* **2002**, *89*, No. 198103.
- (50) Fan, R.; Karnik, R.; Yue, M.; Li, D. Y.; Majumdar, A.; Yang, P. D. DNA Translocation in Inorganic Nanotubes. *Nano Lett.* **2005**, *5*, 1633–1642.

AR040274H